play a role. A very closely related micellar phase composed of disk-shaped micelles can be prepared. This would presumably have very similar surface properties but very different interstitial spaces. It might provide a reasonable test of the relative importance of steric and surface association forces.

The fact that we were able to find an orientation which, when combined with C–D bond vectors taken from the crystal structure, reproduces observed quadrupole splittings is interesting in itself. It also suggests that it is highly likely that the structure of sucrose in a liquid crystal environment is in close agreement with that found in the crystal or in simple solutions. It also suggests that the rather drastic assumption that the molecule executes an axially symmetic motion is not far from correct. This latter suggestion is actually supported by other evidence. Deuterium spectra such as those shown in Figure 3 actually show variations in quadrupole splittings due to variations in the composition of the liquid crystal or variations in the temperature at which the spectra were run. All splittings, with the possible exception of those assigned to deuterons on groups with internal motions (6 and 6′ deuterons), seem to scale with a single order parameter. If motion were not axially symmetric one would require several order parameters to describe motional averaging, and it is unlikely that all of these would respond the same way to environmental changes or have the same effect on all deuterated sites.

In addition to providing structural and motional information, the experiments illustrate some new methodology. In particular, the data illustrate the potential for catalytically labeling molecules and using the differential rates of label incorporation at different sites to make assignments. Although we were able to confirm assignment using chemical shift information in a few cases, our ability to do this may degrade with increasing line widths as we move to larger and larger molecules. The experiments, therefore, significantly enhance the promise that quadrupole coupling data on molecules in oriented media can be of use in the conformation and orientation study of more complex oligosaccharides and membrane systems.

Acknowledgment. This research was supported by a grant from the National Institution of Health (GM 33225) and benefited from instrumentation programs of the National Institute of General Science (GM 32243S1).

Registry No. Sucrose, 57-50-1.

Powder ENDOR Spectra of *p*-Benzoquinone Anion Radical: Principal Hyperfine Tensor Components for Ring Protons and for Hydrogen-Bonded Protons

Pádraig J. O'Malley† and Gerald T. Babcock*

Contribution from the Department of Chemistry, Michigan State University, East Lansing, Michigan 48824-1322. *Received November 18, 1985*

Abstract: ENDOR spectra for the immobilized *p*-benzosemiquinone anion radical ($BQ^{\bullet-}$) in disordered matrices are presented. Hyperfine interactions of the unpaired electron with three different classes of protons are apparent in the spectra and have been investigated: α-proton, hydrogen-bonded proton, and general matrix proton. Dipolar interactions are not averaged in powder samples, and first derivative ENDOR lines are observed for α- and hydrogen-bonded protons at frequencies which correspond to their principal hyperfine tensor values. Interpretation of the spectra has been facilitated by selective deuteration of the parent quinone and of the solvent. The *g* anisotropy of $BQ^{\bullet-}$, although weak, allows orientation selection experiments at X-band which have provided information on the axis directions for the tensor components relative to the molecular structure. Hydrogen bonding of the $BQ^{\bullet-}$ carbonyl group to the alcohol hydroxyl group of the solvent is characterized by a purely dipolar interaction exhibiting axial symmetry. The hydrogen bond direction is in the plane of the quinone ring and the O···H bond distance is calculated to be 1.6 Å. The principal hyperfine tensor components of the α-proton interaction are shown to depend critically on the nearest neighbor carbon spin density values which cause the principal values to deviate substantially from those expected for an isolated $^{\bullet}$C–H fragment. For the unpaired electron spin density distribution in $BQ^{\bullet-}$, the α-proton hyperfine tensor acquires approximately axial character. In the matrix region, several classes of weakly interacting protons contribute to the structured ENDOR line shape observed; orientation selection and selective deuteration have been used to resolve the origin of some of the lines in this region. The observed ENDOR band shapes for each type of proton–electron interaction indicate that the nuclear relaxation probability (ω_n) is independent of orientation.

Since the first demonstration of the ENDOR response in 1956[1] it has been widely used in the analysis of free radical species in both the liquid and the solid state.[2] Recent developments in spectrometer design have demonstrated the feasibility of applying the ENDOR technique to most organic radicals in liquid solution.[3-5] The benefits of this approach are particularly obvious for complex organic molecules (e.g., the chlorophylls) where the large number of hyperfine interactions often leads to an unresolved EPR spectrum. A disadvantage with liquid solution EPR and ENDOR studies, however, is that information on the electron dipole–proton dipole interaction is lost owing to the averaging of this term by the radical tumbling in solution. One usually resorts to single-crystal studies to retrieve this information. Unfortunately, this approach is not feasible in some cases, particularly in biological systems, where only powder samples or disordered solids are available.

The ENDOR spectrum of organic radicals in disordered solids is usually complicated by the broadened nature of the ENDOR response observed.[6] In certain favorable cases, where *g* or hy-

† Present Address: Department of Chemistry, University of Manchester, Institute of Technology, P.O. Box 89, Manchester M60 1QD, UK.

(1) Feher, G. *Phys. Rev.* **1956**, *103*, 834.
(2) Kevan; Kispert, L. D. In *Electron Spin Double Resonance*; Wiley: New York, 1976.
(3) Mobius, K.; Frohling, W.; Lendzian, F.; Lubitz, W.; Plato, M.; Winscom, C. J. *J. Phys. Chem.* **1982**, *86*, 4491.
(4) (a) Lubitz, W.; Lendzian, F.; Mobius, K. *Chem. Phys. Lett.* **1981**, *81*, 235. (b) Kurreck, H.; Bock, M.; Bretz, N.; Elsner, M.; Krans, H.; Lubitz, W.; Muller, F.; Geissler, J.; Kroneck, P. M. *J. Am. Chem. Soc.* **1984**, *106*, 737.
(5) (a) Kurreck, H.; Kirste, B.; Lubitz, W. *Angew. Chem., Int. Ed. Engl.* **1984**, *23*, 173. (b) Mobius, K.; Lubitz, W., submitted.

0002-7863/86/1508-3995$01.50/0

perfine tensor anisotropy is present, it is possible to obtain single crystallike spectra by setting the magnetic field to so-called turning points in the EPR spectrum.[6,7] Generally, the larger the anisotropy the better the orientation selection. However, in the absence of significant anisotropy in the g or hyperfine tensor, as is usually the case for carbon-based organic free radicals, the severe broadening of the spectral response, especially for α-proton interactions, has precluded any in-depth studies. This situation is apparent in the work of Hyde et al.[6a] and of Kwiram and Dalton,[6b,c] who have studied anisotropic hyperfine interactions in powder samples. The former group focused on β-proton couplings, primarily those which arise from rotating methyl groups, while the latter authors investigated both α- and β-proton hyperfine interactions. Although the methyl group interaction, particularly in flavins,[4b,6d,e] and in quinones,[8a] has been studied subsequent to the early work, further characterization of α-proton tensors in powder samples has not been developed.

In a preliminary analysis of quinone free radicals,[8] we have shown that a derivative presentation of the ENDOR response from proton–electron hyperfine interaction results in a clearer resolution of the so-called turning points occurring at the principal values of the hyperfine tensor. The recent improvements in spectrometer design[3] are a major factor in the better resolution attained. In this report we present an account of three types of electron–nuclear hyperfine interactions detectable in the powder ENDOR spectrum of the α-benzosemiquinone anion radical, namely, those which arise from α-protons, from hydrogen-bonded protons, and from general matrix protons. Selective deuteration and theoretical calculations are used in the assignment of the various couplings observed, and orientation selection experiments designed to determine the directional properties of the dipolar interactions are described. The various relaxation mechanisms thought to be contributing to the ENDOR band intensities are also discussed. An account of the application of the methods described here to the biologically important ubiquinone anion radical recently has been presented.[8c]

Experimental Section

The semiquinone anion radical was generated by air oxidation of the corresponding hydroquinone solution (10^{-3} M) in slightly basic isopropyl alcohol or isopropyl alcohol-d. The hydroquinone used was Aldrich reagent grade which was further purified by double sublimation. Perdeuterated benzoquinone was prepared according to the method of Charney and Becker.[9] The EPR and ENDOR spectra were recorded on a Bruker ER 200D spectrometer equipped with a Bruker ENDOR accessory.[10] All spectra were recorded at 123 K unless otherwise stated. The radical EPR spectra were first recorded at 298 K to ensure formation of the correct radical species. The samples were then frozen and stored in liquid nitrogen prior to recording powder ENDOR spectra.

Results

Hydrogen-Bonding Interaction. The proton ENDOR spectrum of immobilized p-benzosemiquinone anion radical in isopropyl alcohol at 123 K is shown in Figure 1a. At least three lines are apparent in the spectrum, and these are labeled a_1, a_2, and a_3; no further splittings with larger hyperfine coupling values were observed in spectra recorded with wider radio frequency ranges. The resonances observed can be assigned by selective deuteration of the isopropyl alcohol solvent and of the ring protons of the benzoquinone radical. The loss of the largest splitting, the a_3 band, in the spectrum of the perdeuterated radical (Figure 1b) demonstrates that this feature is due to hyperfine coupling from the α-protons (interactions involving this set of protons are discussed in detail in the next section). In Figure 1c the ENDOR spectrum of the perdeuterated radical in $(CH_3)_2CHOD$ demonstrates that deuteration of the solvent –OH group results in the loss of the a_1 and a_2 couplings which indicates that these lines are the result of hyperfine coupling between the solvent –OH groups and unpaired spin density of the benzoquinone radical.

The shape of the a_1 and a_2 resonances observed for the solvent protons, remembering that the spectrum is a derivative presentation, is typical of that expected for an axially symmetric tensor with a buildup of intensity at the principal values.[11,12] Although no other analyses of hydrogen-bonded proton–unpaired electron interactions have been described for powder systems, some studies of this kind of interaction in single crystals have been reported.[13] The tensors obtained for such protons have, in general, been shown to be axial and purely dipolar in nature with principal values in the ratio −1:−1:+2. A similar situation can be expected for the p-benzosemiquinone anion radical. The largest and positive value

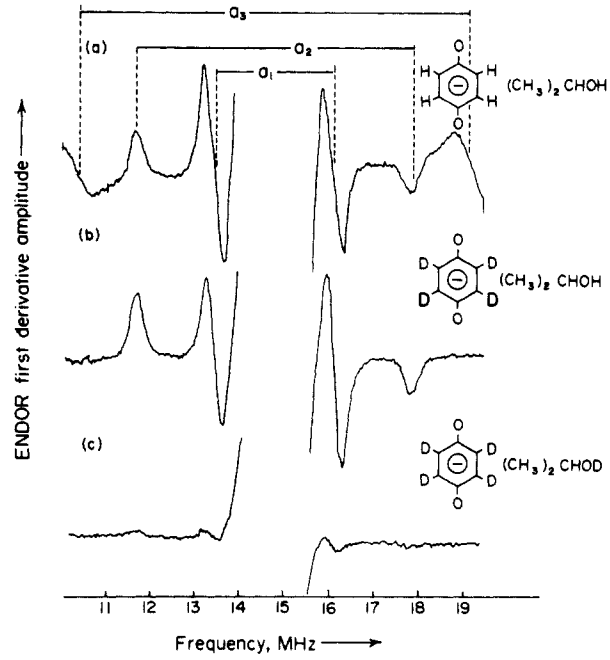

Figure 1. ENDOR spectra for (a) p-benzosemiquinone anion radical in isopropyl alcohol (temperature, 123 K; microwave power 1 mW; radio frequency power at 10 MHz, 50 W; fm deviation, ±150 kHz), (b) perdeuterated p-benzosemiquinone anion radical in isopropyl alcohol (temperature, 123 K; microwave power 1 mW; radio frequency power at 10 MHz, 45 W; fm deviation, ±150 kHz), (c) perdeuterated p-benzosemiquinone anion radical in isopropyl alcohol-d (temperature, 123 K; microwave power, 1 mW; radio frequency power at 10 MHz, 45 W; fm deviation, ±150 kHz).

Table I. Hyperfine Tensor Components (in MHz) for the p-Benzosemiquinone Anion Radical in Isopropyl Alcohol

protons	A_{xx}	A_{yy}	A_{zz}	A_{iso}
H bonded	+5.9	−2.8	−2.8	+0.1
α[a]	−10.2	−3.9	−9.0	−7.7
	(−10.5)	(−2.4)	(−10.2)	(−7.7)

[a] Values in parentheses indicate calculated values, see text.

(6) (a) Hyde, J. S.; Rist, G. H.; Ericksson, L. E. G. *J. Phys. Chem.* **1968**, *72*, 4269. (b) Kwiram, A. L. *J. Chem. Phys.* **1968**, *49*, 2860. (c) Dalton, L. R.; Kwiram, A. L. *J. Chem. Phys.* **1972**, *57*, 1132. (d) Eriksson, L. E. G.; Hyde, J. S.; Ehrenberg, A. *Biochim. Biophys. Acta* **1969**, *192*, 211. (e) Eriksson, L. E. G.; Ehrenberg, A. *Biochim. Biophys. Acta* **1973**, *293*, 57.

(7) (a) Allendoerfer, R. D. *Chem. Phys. Lett.* **1982**, *17*, 172. (b) Rist, G. H.; Hyde, J. S. *J. Chem. Phys.* **1970**, *52*, 4633. (c) Scholes, C. P.; Isaacson, R. A.; Feher, G. *Biochem. Biophys. Acta* **1982**, *263*, 448. (d) Schweiger, A. W. *Struct. Bonding* **1982**, *51*, 1. (e) Hurst, G. C.; Henderson, T. A.; Kreilick, R. W. *J. Am. Chem. Soc.* **1985**, *107*, 7294. (f) Henderson, T. A.; Hurst, G. C.; Kreilick, R. W. *J. Am. Chem. Soc.* **1985**, *107*, 7299.

(8) (a) O'Malley, P. J.; Babcock, G. T. *J. Chem. Phys.* **1984**, *80*, 3912. (b) O'Malley, P. J.; Babcock, G. T. *J. Am. Chem. Soc.* **1984**, *106*, 817. (c) O'Malley, P. J.; Chandrashekar, T. K.; Babcock, G. T. In *Antennas and Reaction Centers of Photosynthetic Bacteria*; Michele-Beyerle, M. E., Ed.; Springer-Verlag: Berlin, 1985; p 339.

(9) Charney, E.; Becker, E. D. *J. Chem. Phys.* **1965**, *42*, 910.

(10) O'Malley, P. J.; Babcock, G. T. *Proc. Natl. Acad. Sci. U.S.A.* **1984**, *81*, 1098.

(11) Ingram, D. J. E. In *Free Radicals*; Butterworths: London, 1958; pp 102–134.

(12) Atkins, P. W.; Symons, M. C. R. In *The Structure of Inorganic Radicals*; Elsevier Publishing Co.: Amsterdam, 1967; p 270.

(13) (a) Muto, H.; Iwasaki, M. *J. Chem. Phys.* **1973**, *59*, 4821. (b) Reddy, M. V. V. S.; Lingam, K. V.; Gundu Rao, T. K. *J. Chem. Phys.* **1982**, *76*, 4398.

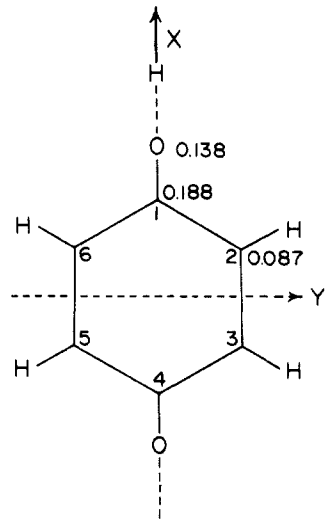

Figure 2. Spin density distribution for the *p*-benzosemiquinone anion radical according to ref 17.

would be expected to lie along the O···H bond, and hence we assign the a_2 value of +5.9 MHz to this dipolar interaction. Taking this value as positive, we then attribute a value of −2.8 MHz (a_1) to the other two directions (Table I).

In the single crystal work on hydrogen-bonded proton–unpaired electron interaction in organic radicals,[13] the assignment of the principal directions of the hyperfine tensor to the molecular axes is facilitated by the direction cosines one obtains in such measurements. For powder spectra, of course, one loses this advantage and the orientation of the hydrogen-bonded proton hyperfine tensor relative to the molecular axes or to the *g* tensor must be determined by other means. On the basis of the increased line width observed in protic solvents, Hales[14] proposed a large hydrogen-bonding interaction for *p*-benzosemiquinone in protic solvents. A hydrogen-bonding direction, as outlined in Figure 2, was postulated with an angle for the C—O···H bond of 180°. Moreover, in Q-band EPR studies, Hales also showed that the principal *g* values for the *p*-benzosemiquinone anion radical are g_x = 2.0065, g_y = 2.0053, and g_z = 2.0023, where the *x* and *y* axes are as defined in Figure 2 and the *z* axis is perpendicular to the aromatic ring plane.[15] The g_z component is significantly different from the two other values, and radicals with a *z*-axis orientation contribute most strongly to the high field side of the immobilized radical EPR spectrum. Therefore, by recording the ENDOR spectrum at a higher field value (field position A in Figure 3), one can effectively minimize contributions from the *x* and *y* directions and only those hyperfine interactions lying along the *z* direction should contribute to the ENDOR spectrum. In Figure 3b the ENDOR spectrum obtained by monitoring EPR field position A shows that only the a_1 band is observed; the absence of the a_2 band in the ENDOR spectrum of Figure 3b shows that the O···H bond direction lies parallel to the ring plane. The ENDOR spectrum recorded on the low-field side of the EPR spectrum (position B) is shown in Figure 3c. Because of the fairly close overlap of g_x and g_y values, orientation selection such as that above for g_z is not possible for these principal directions at X-band, and the ENDOR spectrum at position B is expected to correspond to the powder spectrum of Figure 3a minus the *z*-component spectrum of Figure 3b. Taking into account the fact that the ENDOR intensities obtained by recording at field positions A and B will not be as strong as that obtained for the zero crossing, it is apparent that this is the case.

In solution, hyperfine interaction between the unpaired electron of the quinone free radical and the hydrogen-bonded solvent proton is not observed, as expected for a purely dipolar interaction. The

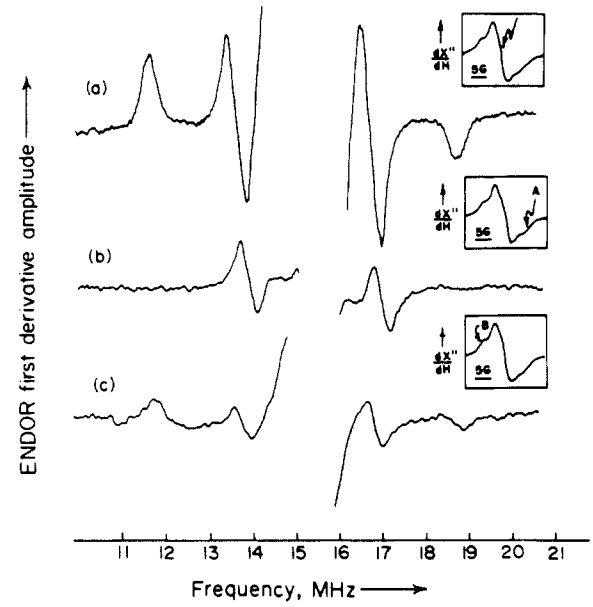

Figure 3. Variation in the ENDOR spectrum of the perdeuterated benzosemiquinone anion radical in isopropyl alcohol as a function of magnetic field monitoring position: (a) temperature, 123 K; microwave power, 1 mW; radio frequency power at 10 MHz, 45 W; fm deviation, ±150 kHz; inset—EPR field monitoring position; (b) temperature, 123 K; microwave power, 1 mW; radio frequency power at 10 MHz, 30 W; fm deviation, ±150 kHz; inset—EPR field monitoring position; (c) temperature, 123 K; microwave power, 1 mW; radio frequency power at 10 MHz, 30 W; fm deviation, ±150 kHz; inset—EPR field monitoring position.

axial hyperfine tensor we observe for this coupling in our powder samples, as well as similar axial tensors observed in the single-crystal work, is expected if the interaction exhibits characteristics of a classical dipole/dipole interaction.[16] Then the *i*th component of the hyperfine tensor (A_i, $i = x, y, z$) can be equated to

$$A_i = 78.4\rho\frac{[3\cos^2\theta - 1]}{r^3} \qquad (1)$$

where A_i is expressed in MHz, ρ is the unpaired electron spin density on the atom to which the proton is hydrogen bonded, θ_i is the angle between the applied magnetic field ($i = x, y, z$) and the line joining the unpaired electron and the hydrogen-bonded proton, and *r* is the distance vector in Å between electron spin and nuclear spin.[11] The spin density distribution for the *p*-benzosemiquinone radical in protic solvents has been described by Sullivan et al.[17] and is outlined in Figure 2. Although the C_1 spin density is somewhat larger than the oxygen spin density, the former would not be expected to contribute substantially (<20%) to the dipole–dipole interaction owing to the r^{-3} dependence. Using the oxygen spin density value of Figure 2 then, one obtains a value for *r* of 1.54 Å for A_{xx} = 5.9 MHz, θ = 0° and 1.57 Å for $A_{yy} = A_{zz}$ = −2.8 MHz, θ = 90°. These values are in good agreement with previously calculated hydrogen-bonded proton–oxygen distances.[18]

(14) Hales, B. J. *J. Am. Chem. Soc.* **1976**, *98*, 7350.
(15) Hales, B. J. *J. Am. Chem. Soc.* **1975**, *97*, 5993.
(16) Wertz, J. E.; Bolton, J. R. *Electron Spin Resonance*: Elementary Theory *and Practical Applications*; McGraw-Hill: New York, 1972.

(17) Sullivan, P. D.; Bolton, J. R.; Geiger, W. E., Jr. *J. Am. Chem. Soc.* **1970**, *92*, 4176. More recent calculations have appeared for the π-electron spin density distribution in benzoquinone anion radicals (e.g., ref 21c). These differ from those of Sullivan et al., particularly in the oxygen spin densities and also in the non-oxygen bound ring carbon densities. We have found, however, that the Sullivan et al. calculation provides a better description of the experimental α-proton couplings, and, accordingly, we have used these results in the calculations described here (see also Silver, B. L. *Theor. Chim. Acta (Berlin)* **1967**, *9*, 192). It is apparent that more extensive calculations are required to describe the spin density distribution in $BQ^{\bullet-}$, and these calculations are now underway.
(18) Vinogradov, S. N.; Linnel, R. H. In *Hydrogen Bonding*; Van Nostrand Reinhold Co.: New York, 1971; p 178. Owing to uncertainties in the precise spin density distribution (see ref 17), we have not carried the distance calculations beyond the point dipole level. A more detailed treatment, along the lines presented below for the α-proton, must await the results of the spin density distribution calculations now in progress.

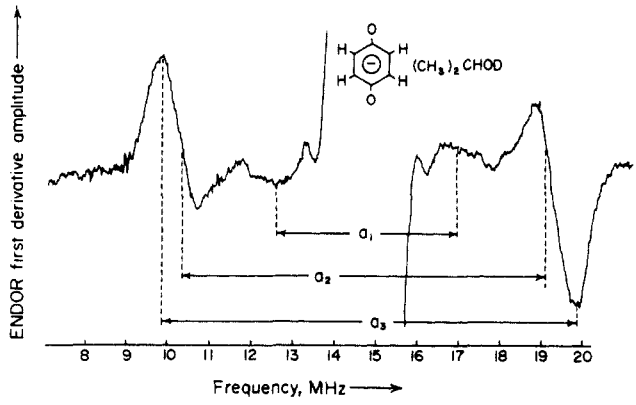

Figure 4. ENDOR spectrum of protonated *p*-benzosemiquinone anion radical in isopropyl alcohol-*d* (temperature, 123 K; microwave power, 1 mW; radio frequency power at 12 MHz, 60 W; fm deviation, ±150 kHz).

α-Proton Interaction. Owing to their high anisotropy, α-proton ENDOR bands have been generally assumed to be of too weak intensity to be observed in powder ENDOR spectra, although they were studied by Kwiram in malonic acid powders as early as 1968.[6b] The a_3 band in Figure 1 and its assignment to α-proton hyperfine coupling clearly demonstrate that ENDOR bands of substantial intensity may be observed from ring protons in the benzoquinone anion radical. We have investigated the hyperfine interactions between the α-protons and the unpaired spin density in the ring in more detail by recording ENDOR spectra of the protonated semiquinone anion in $(CH_3)_2CHOD$ (Figure 4). Removal of the strong hydrogen-bonded proton resonances reveals an underlying weak and fairly broad ENDOR line due to the α-protons which is denoted as a_1 in Figure 4. By recording the spectrum with low radio frequency modulation amplitude, higher resolution of the spectrum can be obtained and, as is apparent in Figure 5a, the a_3 resonance of Figure 1 is shown to be composed of two closely overlapped lines which we denote as a_2 and a_3. We conclude that the α-protons of the benzoquinone anion radical show a powder ENDOR spectrum with three resolved resonances. Thus, similar to the hydrogen-bonded proton resonances of the previous section and to the quinone methyl group interactions described previously,[8a] the hyperfine interaction with α-protons produces an ENDOR spectrum which, although spread over a considerable radio frequency range, has reasonably well-resolved turning points which correspond to the principal values of the hyperfine tensor. The absolute values of these components as determined from Figures 4 and 5a are 3.9, 9.0, and 10.2 MHz.[19]

For α-protons we expect that the sign of the isotropic hyperfine coupling will be negative.[16] We use this plus the solution measurements of Hyde[20] which showed a fairly large isotropic coupling for the α-protons of benzosemiquinone anion to assign the three observed hyperfine tensor components of these protons as negative. These values are listed in Table I along with the isotropic hyperfine coupling, −7.7 MHz, which is obtained from the tensor components. The sign and magnitude of this isotropic coupling are consistent with those expected for the semiquinone anion α-proton hyperfine interaction and support the assignment of signs for the tensor components in Table I. The difference between this value and the −6.7 MHz value measured by Hyde[20] (which we confirmed in room temperature solution experiments for benzoquinone anion radical in isopropyl alcohol) most likely arises from slight shifts in unpaired spin density distribution as the solution is frozen and the hydrogen bonds immobilized.[21]

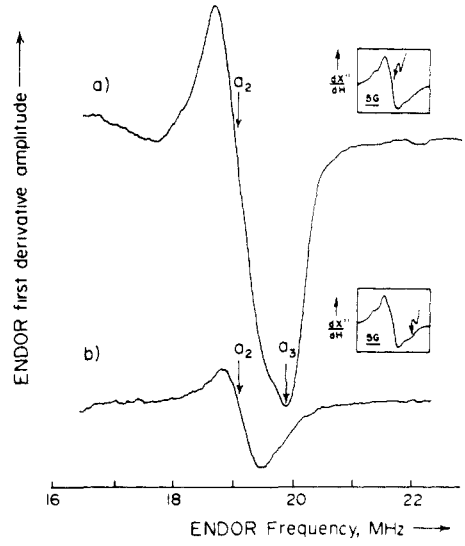

Figure 5. Variation of the ENDOR spectrum for the protonated *p*-benzosemiquinone anion radical in isopropyl alcohol-*d* as a function of the EPR monitoring field. ENDOR conditions: temperature, 123 K; microwave power, 1 mW; radio frequency power at 10 MHz, 45 W; fm deviation, ±150 kHz.

The observed hyperfine tensor for the anion radical α-protons (Table I) shows nearly axial symmetry. At first glance, this is unusual as one expects that the hyperfine tensor components for an isolated •C–H fragment will occur at frequencies corresponding to $0.5a_{iso}$, $1.0a_{iso}$, and $1.5a_{iso}$.[6b,22] To rationalize the situation, we use the calculated spin densities of Figure 2 which indicate that there is substantial unpaired spin density at the 1,4-carbon positions, roughly twice that at the α-proton carbon positions, as well as at the two para oxygens. We anticipate that dipole–dipole interactions between these nonbonded carbons and oxygens will contribute to the observed (net) α-proton dipolar tensor. This kind of situation has been encountered in aromatic radicals by previous workers (e.g., ref 23) and considered in detail by Heller and Cole for allyl-type free radicals.[24] We adopt their approach below in order to interpret the approximately axial hyperfine tensor for the α-protons of the benzosemiquinone anion radical.

Electron–nuclear dipolar interaction between the α-proton at the ring 2 position and unpaired electron spin density at four atoms, C_1, C_2, C_3, and the para O, are expected to contribute to the measured dipolar hyperfine tensor. To determine this tensor, $\mathbf{A}^T$, we sum the four individual dipolar tensors which result from the interaction of the proton with the unpaired spin density at each of the four atoms, i.e.,

$$\mathbf{A}^T = \sum_{k=1}^{4} \mathbf{A}^k \qquad (2)$$

where $\mathbf{A}^k$ is the dipolar tensor for the proton–*k*th atom unpaired electron spin density interaction. To carry out the tensor addition process we write each of the tensors in their respective principal axis systems, rotate each to a common axis system, carry out the addition, and finally diagonalize to obtain the principal values of $\mathbf{A}^T$ and the direction of its axis system with respect to the ring system.

(a) Spin Density at Carbon C_2. The form of the dipolar tensor for this interaction is expected to have that of an isolated C–H fragment with the values of the tensor components determined by the spin density at C_2 and the length of the C–H bond. The latter is taken as 1.088 Å.[23,24] With this bond distance and an unpaired spin density of 1.0, a tensor with $A_{xx} = -32$ MHz, A_{yy}

(19) These values differ from those we assigned originally for the *p*-benzosemiquinone anion radical.[8b] In the earlier, preliminary analysis, the a_2 band of Figure 1 was attributed to the α-proton interaction on the basis of theoretical calculations for an isolated •C–H fragment. The deuteration experiments of Figure 1 clearly show, however, that this band corresponds to the $A_{\parallel}$ component of the hydrogen-bonded proton interaction.

(20) Hyde, J. S. *J. Chem. Phys.* **1965**, *43*, 1806.

(21) (a) Gendell, J.; Freed, J. H.; Fraenkel, G. K. *J. Chem. Phys.* **1962**, *37*, 2832. (b) Zandstra, P. J. *J. Chem. Phys.* **1964**, *41*, 3655. (c) Spanget-Larsen, J. *Theor. Chim. Acta (Berlin)* **1978**, *47*, 315.

(22) (a) McConnell, H. M.; Heller, C.; Cole, T.; Fessenden, R. W. *J. Am. Chem. Soc.* **1960**, *82*, 766. (b) Pooley, D.; Whiffen, D. H. *Mol. Phys.* **1961**, *4*, 81. (c) Horsfield, A.; Morton, J. K.; Whiffen, D. H. *Mol. Phys.* **1961**, *4*, 169.

(23) (a) Hirota, N.; Hutchison, C. A., Jr.; Palmer, P. *J. Chem. Phys.* **1964**, *40*, 3717. (b) Bohme, U. R.; Wolf, H. C. *Chem. Phys. Lett.* **1972**, *17*, 582.

(24) Heller, C.; Cole, T. *J. Chem. Phys.* **1962**, *37*, 243.

= +32 MHz, and A_{zz} = 0.0 has been determined for prototype •C–H fragments in dicarboxylic acids where the direction of A_{yy} is along the •C–H bond and the direction of A_{zz} is perpendicular to the molecular plane.[22] Adapting this to the C_2–H fragment with ρ_c = 0.087 (Figure 2), we obtain the following principal tensor components:

$\mathbf{A}^{C_2}$:

$$A_{xx} = -2.8 \text{ MHz}; A_{yy} = 2.8 \text{ MHz}; A_{zz} = 0$$

(b) Spin Density at Carbon C_1. The dipolar tensor for this interaction can be determined in two different ways. If a point dipole approximation is used, the tensor components can be calculated in a straightforward manner by using eq 1. If the validity of this approximation is questionable, the procedure developed by McConnell and Strathdee[25] must be used. We follow the latter course by assuming a C_1–C_2 bond distance of 1.4 Å[23,24] which yields a C_1···H distance of 2.16 Å. Substituting this value into the McConnell–Strathdee equations with ρ = 0.188 (Figure 2) produces the following hyperfine tensor

$\mathbf{A}^{C_1}$:

$$A_{xx} = -1.5 \text{ MHz}; A_{yy} = +2.8 \text{ MHz}; A_{zz} = -1.3 \text{ MHz}$$

with the A_{yy} direction along the C_1···H direction and A_{zz} perpendicular to the quinone plane. Interestingly, the tensor obtained by the point dipole approximation is almost the same ($A_{xx} = A_{zz}$ = −1.45; A_{yy} = +2.9 MHz), which indicates that at this distance the effects of electron delocalization become minimal. Straightforward geometric considerations show that the angle between the A_{yy} directions for $\mathbf{A}^{C_2}$ and $\mathbf{A}^{C_1}$ is 34.1°. Rotation of $\mathbf{A}^{C_1}$ into the axis system of $\mathbf{A}^{C_2}$ produces the $\mathbf{A}^{C_1'}$ tensor.

(c) Spin Density at Carbon C_3. C_3 is related to C_1 by a 180° rotation about the C_2–H axis, and its hyperfine tensor is obtained by scaling the C_1 tensor according to the difference in spin density. The resulting principal values are

$\mathbf{A}^{C_3}$:

$$A_{xx} = -0.69 \text{ MHz}; A_{yy} = 1.29 \text{ MHz}; A_{zz} = -0.6 \text{ MHz}$$

with A_{yy} along the C_3···H direction. The angle between the A_{yy} directions for $\mathbf{A}^{C_2}$ and $\mathbf{A}^{C_3}$ is ~34.1°. Rotation of $\mathbf{A}^{C_3}$ into the axis system of $\mathbf{A}^{C_2}$ produces the $\mathbf{A}^{C_3'}$ tensor.

(d) Spin Density at Oxygen O_1. Given the results above regarding the suitability of the point dipole approximation in determining $\mathbf{A}^{C_1}$, we have used eq 1 to calculate $\mathbf{A}^{O}$. For a semiquinone anion, the carbon–oxygen bond distance is uncertain,[26] and we have used as an estimate a value of 1.4 Å. The calculations are not extremely sensitive to this distance. The distance between the oxygen and the α-proton at C_2 is then determined to be 2.66 Å, and the tensor is

$\mathbf{A}^{O}$:

$$A_{xx} = -0.57 \text{ MHz}; A_{yy} = 1.15; A_{zz} = -0.57 \text{ MHz}$$

where A_{yy} is along the O···H direction and A_{zz} is perpendicular to the ring plane. When rotated into the $\mathbf{A}^{C_2}$ axis system (θ = 58.2°), $\mathbf{A}^{O'}$ is obtained.

The four tensors may now be summed in order to obtain $\mathbf{A}^{T}$ which in turn is diagonalized to produce the following principal tensor components:

$\mathbf{A}^{T}$:

$$A_{xx} = -2.8 \text{ MHz}; A_{yy} = 5.3 \text{ MHz}; A_{zz} = -2.5 \text{ MHz}$$

The direction of the A_{yy} is rotated by 14° away from the C_2–H axis toward the y axis in Figure 2. When $\mathbf{A}^{T}$ is combined with the experimental value of A_{iso} = −7.7 MHz, the principal hyperfine tensor components shown in Table I are obtained. Reasonable agreement with the experimental values is observed as the calculated tensor is approximately axial and A_{yy} is the least negative component. Given the approximate nature of the molecular orbital calculations which led to the spin density distribution of Figure 2, we consider the agreement as satisfactory.[17]

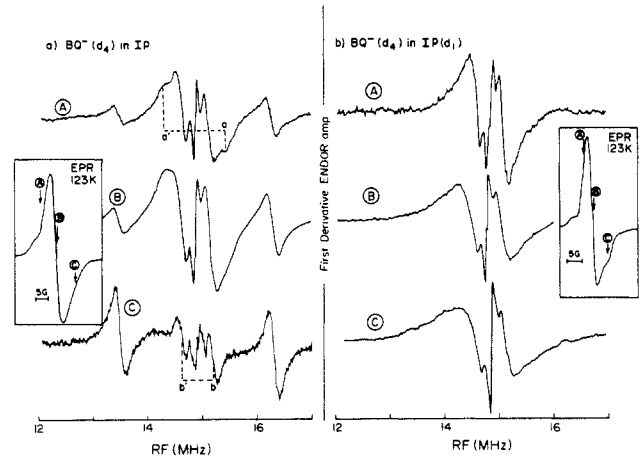

Figure 6. Matrix ENDOR spectra of perdeuterated $BQ^{\bullet-}$ in (a) isopropyl alcohol and in (b) isopropyl alcohol-*d* as a function of magnetic field. ENDOR conditions: temperature, 123 K; microwave power, 6.3 mW; radio frequency power at 12 MHz, 120 W; fm deviation, ±30 kHz; number of scans, 20; time constant, 0.5 s. Insets: EPR spectra and monitoring fields.

Two additional points can be made regarding the calculated and observed α-proton hyperfine tensor. First, in simulating the EPR spectrum of benzosemiquinone anion, Hales found that an approximately axial α-proton tensor oriented along the x,y axis system of Figure 2 reproduced the experimental spectrum reasonably well.[15] Although we have arrived at the "axial" tensor of Table I with an orientation close to the x,y axis system in Figure 2 by completely different arguments, the simulation results he obtained are consistent with our conclusions regarding the nature of this tensor. Second, because we are dealing with powder samples, the assignment of the directions of the experimental tensor components in Table I is based on the general properties of α-proton hyperfine tensors (e.g., the smallest principal hyperfine component is expected to be approximately in the direction of the C–H bond) and on the agreement with the calculated tensor components.

We have put these assignments on more solid ground by taking advantage of the g anisotropy of the benzoquinone anion radical. In Figure 5b, the ENDOR spectrum recorded while monitoring at EPR field position A (see inset) is illustrated. As indicated in the previous section this procedure selects only those molecules which have their aromatic ring planes perpendicular to the magnetic field. One therefore expects to observe an ENDOR band corresponding to the hyperfine component along the z direction. Figure 5b shows that only the a_2 component is observed which confirms the assignment of the −9.0 MHz coupling to the A_{zz} component. Repeating this experiment with the magnetic field set to the low-field side of the EPR spectrum eliminates a_2 from the ENDOR spectrum and only a_1 and a_3 are seen (not shown), in agreement with the in-plane directions assigned for these two hyperfine tensor components in Table I.

Matrix Proton Interactions. The observation of a broad band at the free nuclear frequency in powder ENDOR spectra has been generally attributed to purely dipolar coupling between the electron spin and nearby protons. Various line shape models have been discussed for this band, which is usually the most intense in the powder spectrum.[6a,27,28] The matrix band observed for the *p*-

(25) McConnell, H. M.; Strathdee, J. *Mol. Phys.* **1959**, *2*, 129.
(26) Trotter, J. *Acta Crystallogr.* **1960**, *13*, 86. For neutral benzoquinone the C=O distance is 1.22 Å, but this bond length is likely to increase upon reduction to form the anion radical.

(27) (a) Leniart, D. S.; Hyde, J. S.; Vedrine, J. C. *J. Phys. Chem.* **1972**, *76*, 2079. (b) Vedrine, J. C.; Hyde, J. S.; Leniart, D. S. *J. Phys. Chem.* **1972**, *76*, 2087. (c) Iwasaki, M.; Muto, H.; Eda, B.; Nunone, K. *J. Chem. Phys.* **1972**, *56*, 3166.

benzosemiquinone radical does not, however, consist of a weakly featured band centered at the free proton frequency. Instead, we have found that this spectral region contains detailed, orientation-dependent structure which is accentuated by the first derivative representation. Figure 6, left panel, shows ENDOR spectra for deuterated $BQ^{\bullet-}$ in protonated isopropyl alcohol and, right panel, for deuterated $BQ^{\bullet-}$ in isopropyl alcohol in which the –OH proton has been replaced by deuterium. The inset in each panel shows the EPR spectrum of the sample and indicates the fields at which the various spectra were recorded. In Figure 6a, the hyperfine resonances for the hydrogen-bonded proton are apparent as the intense, derivative-shaped lines at 13.5 MHz and 16.3 MHz (see above); their intensity variation, relative to the intensity of the matrix region peaks, with magnetic field setting for the various spectra provides an indication of the orientation selection achieved in the experiment.

In most line shape analyses of the matrix region (e.g., ref 27), the spectrum is considered to have contributions from two, somewhat artificially, distinguished classes of protons: "close" protons lie within 4–5 Å of the radical and have small but finite isotropic couplings, in addition to anisotropic interactions, with the unpaired electron spin; "far" protons are at distances greater than 5 Å and have only weak dipolar coupling. Because the "far" protons are only minimally perturbed by the radical, their Larmor frequency is close to the free proton frequency and they contribute only to the center of the matrix region around ν_p. The "close" protons, owing to their larger hyperfine interaction, dominate in the wings of the spectrum. In the line shape analysis of Hyde, Leniart, et al.,[6a,27a,b] the matrix response is generally considered to be proportional to T_{1n}^{-1}, the nuclear spin lattice relaxation time, and this is usually taken to be orientation independent (e.g., ref 28c). Narayana, Kevan, and co-workers[28] have refined this analysis by eliminating several assumptions inherent in the ideal line shape theory and have included explicity the radio frequency and microwave field dependencies of the matrix response. In their most recent work,[28d] they point out the importance of angularly independent nuclear spin diffusion effects in determining the nuclear relaxation rate and identify this phenomenon as controlling the behavior of the matrix signal. The results of this analysis are in good agreement with the earlier ideal line shape analysis (discussed most extensively in ref 28b).

The results in Figure 6b for $BQ^{\bullet-}$ in $IP(d_1)$ are generally consistent with this analysis. The coupling of ~150 kHz is typical[2,27a] of the double-peaked matrix response characteristic of protons with an angularly independent T_{1n}^{-1}; the broader resonance with a nominal coupling of ~525 kHz is generally observed for the "close" protons.[28] The latter band is clearly composed of various underlying peaks which we have not resolved even at very low modulation amplitude values and at low (<10 K) temperatures. We anticipate that the delocalization of the electron spin over the carbon and oxygen atoms of the quinone will further complicate this region.

When the solvent is fully protonated, the matrix region develops additional features (Figure 6, left panel). Two new resonances, labeled *a* and *b*, are observed at 1.14 and 0.59 MHz, respectively. Resonance *a* is most clearly observed at low field where molecules with their rings parallel to the laboratory field are selected, whereas resonance *b* is most pronounced at high field where perpendicular orientations are favored. This orientation dependence, the axial character of the shapes of the two resonances, and the fact that $a = 2b$ are analogous to the characteristics of the strongly hydrogen-bonded proton discussed above. These similarities indicate that the *a*, *b* resonances arise from a dipolar-coupled solvent hydroxyl proton with an isotropic hyperfine interaction of essentially zero; the $\theta = 0$ axis for the dipolar–dipole interaction apparently lies in the plane of the quinone ring. There is evidence from IR spectroscopy for two classes of hydrogen bonds to quinones,[29] one strong and the other weak, and the proton responsible for the *a*, *b* resonances in Figure 6 may belong to the second, weakly bound class. Assuming that the proton is bonded to the quinone oxygen and using eq 1, we calculate an H···O distance of 2.67 Å. Whether a hydrogen at this distance actually interacts sufficiently strongly with the oxygen to be detected in the IR spectrum is uncertain. What does appear to occur, however, is that hydroxyl protons from the solvent assume a well-defined geometry with repect to the radical with this separation distance.

Discussion

The above results demonstrate the feasibility of extracting the principal hyperfine interaction values from the turning points of a powder ENDOR spectrum for α-protons and hydrogen-bonded protons. Combined with similar results on rotating methyl groups obtained by us[8,30] and others,[6,7] this provides a simple method for determining the principal hyperfine tensor components for various aromatic radicals with ring proton and methyl substituents as well as for exploring the interaction of the radical with its local solvent environment. As with *g*-tensor analyses of powder EPR spectra, a drawback with this technique is that the directional properties of the principal axes cannot be directly determined from the spectra. However, as demonstrated in Figures 3 and 5, recording the ENDOR response from different portions of the EPR spectrum and combining the results with calculation of the expected hyperfine tensor[24,25] can be helpful in this regard. As originally noted by Dalton and Kwiram,[6c] orientation selection in powder spectra will produce single-crystal-type spectra, rather than powder spectra, as long as cross relaxation is slow relative to T_{1e}. For organic radicals, this condition appears to be met, provided the temperature is not too low. Hoffman and co-workers have recently presented a general formulation for powder ENDOR spectra recorded under these conditions.[31] Although their focus is on metalloprotein ENDOR where *g*-anisotropy is usually very pronounced, the principles should be applicable to the organic radical case as well.

For the α-proton of $BQ^{\bullet-}$, our data show that the hyperfine tensor is approximately axial. The overall anisotropy is significantly less than expected on the basis of single-crystal work on $^{\bullet}C-H$ fragments;[22] such a situation facilitates ENDOR detection of the turning points in the spectrum. We attribute this behavior to the delocalized nature of the aromatic $BQ^{\bullet-}$ and the resulting nearest neighbor contributions to the electron dipole–nuclear dipole interaction. As with β-protons, nearest-neighbor effects on α-proton tensors introduce axial character to the principal components. A second effect of these nearest-neighbor interactions is to cause the axis system of the α-proton hyperfine tensor to deviate from that expected for isolated $^{\bullet}C-H$ fragments, i.e., a principal direction is no longer necessarily colinear with the C–H bond direction. Only if the spin density distribution in the radical is symmetric with respect to this bond do we expect no shift in the tensor axis directions. An example of this latter case is the work by Heller and Cole on allyl-type free radicals.[24]

Neighboring spin density contributions to the α-proton tensor observed here for $BQ^{\bullet-}$ appear to be general to aromatic radicals. For example, in the tyrosine free radical in the enzyme, ribonucleotide reductase, the 3,5 ring protons have a substantial isotropic hyperfine interaction,[32a] and ENDOR results we have obtained show that the dipolar contributions to the overall hyperfine tensor again are at variance with the isolated C–H fragment case.[32b] The α-proton anisotropic hyperfine tensors should provide a useful measure of the spin density distribution in the ring and the effects of the local environment of the radical on this distribution.

(28) (a) Narayana, P. A.; Bowman, M. K.; Becker, D.; Kevan, L.; Schwartz, R. N. *J. Chem. Phys.* **1977**, *67*, 990. (b) Kevan, L.; Narayana, P. A.; Toriyama, K.; Iwazaki, M. *J. Chem. Phys.* **1979**, *70*, 5006. (c) Kevan, L.; Narayana, P. In *Multiple Electron Resonance Spectroscopy*; Dorio, M. M., Freed, J. H., Eds.; Plenum Press: New York, 1979; pp 229–259. (d) Schlick, S.; Kevan, L.; Toriyama, K.; Iwazaki, M. *J. Chem. Phys.* **1981**, *74*, 282.

(29) Fritzsche, H. *Z. Phys. Chem.* **1966**, *43*, 154.

(30) O'Malley, P. J.; Babcock, G. T., to be submitted.

(31) Hoffman, B. M.; Martinsen, J.; Venters, R. A. *J. Magn. Reson.* **1984**, *59*, 110.

(32) (a) Reichard, P.; Ehrenberg, A. *Science* **1983**, *221*, 514. (b) Chandrashekar, T. K.; Barry, B.; Babcock, G. T.; Salowe, S. P.; Stubbe, J., unpublished.

The ability to extract information on the hydrogen bonds to the carbonyl groups of the quinone from powder ENDOR has also been demonstrated. Solvent perturbations of semiquinones in hydroxylic solvents have been noted for some time, and variations in the hyperfine splitting of the α-proton as well as in g-value have been observed in going from hydroxylic to nonhydroxylic solvents.[21] Gendell et al.[21a] postulated that the formation of H-bonded complexes in liquid solution resulted in a redistribution of the π-electron spin density hence giving rise to the variation in hyperfine splitting observed in various solvents. A two-site model for the hydrogen-bonding interaction was proposed. Hydrogen bonding between the quinone carbonyls and the hydroxyl group of the solvent has also been proposed by Yonezawa et al.[33] to alter the isotropic g factor for the p-benzosemiquinone anion radical. To explain their results, these workers proposed a four-site model for hydrogen bonding.

The above studies were all performed in liquid solution where no direct evidence for H bonding, such as extra hyperfine splitting from the H-bonded proton, could be detected. Observation of a small isotropic splitting (see Table I) from the H-bonded proton might indeed be expected as the observation of alkali metal ion pair splittings is common.[16] However, the absence of significant hyperfine splitting in the liquid solution spectra can be explained by assuming that the lifetime of the H-bonded complex is short thereby resulting in an averaging of the proton splitting to zero.[21a] Hales[15] showed that by recording the EPR spectrum in frozen matrices the H-bonding interaction manifests itself as a broadening of the EPR line width in protic solvents. His data also supported the two-site H-bonding model proposed by Gendell et al.[21a] and Stone and Maki.[34] The increased resolution inherent in the ENDOR technique now allows us to measure directly the hyperfine splitting from the H-bonded protons. The hyperfine interaction is shown to be essentially dipolar in nature, and the broadening of the EPR signal observed in protic frozen matrices by Hales[15] can be attributed to the "freezing in" of this dipolar term. The dipole–dipole interaction between the hydroxyl proton of the solvent and the electron spin density on the oxygens of the quinone radical allows us to estimate the H···O bond length to be 1.6 Å. The ENDOR approach represents a unique method of obtaining hydrogen-bonding distances as X-ray crystal-structure determinations of H···B bond lengths is often infeasible.[18]

Feher, Lubitz, and co-workers,[35] have recently applied these principles[8c] to powder ENDOR characterization of the bound ubiquinone acceptors in the reaction center complex from photosynthetic bacteria. In a versatile approach to this problem, they used both deuterium and ^{17}O isotropic substitution to demonstrate that the two carbonyl oxygens of the first quinone acceptor form hydrogen bonds of unequal strength; for the second quinone acceptor their data indicate two approximately equal hydrogen bonds. From the axial hyperfine tensors for the hydrogen-bonded protons they estimated distances for the various bonds they observed.

A general description of the types of powder ENDOR band shapes expected, assuming various mechanisms for the nuclear relaxation, has been outlined by Lenniart et al.[27] The shapes of the ENDOR bands observed in this study for α-proton and hydrogen-bonded proton interaction and in our investigation of rotating methyl groups[30] clearly indicate that Case 1 of ref 27 is applicable. In this situation, the nuclear relaxation probability (ω_N) is assumed to be independent of orientation, which suggests that a rotationally invariant mechanism is responsible for the nuclear relaxation. Qualitatively, this implies that the dependence of the powder ENDOR band shape on orientation should be similar to that observed for EPR powder band shapes,[12] as is indeed the case.

We have also noted that the ENDOR response from the H-bonded protons is very strong in comparison with that obtained from the α-protons. Even when 98% deuterated $(CH_3)_2CHOD$ is used, trace bands due to the H-bonding proton can be observed (Figure 1c). The ENDOR response is generally assumed to be directly proportional to the ω_N value of the proton concerned.[36] This therefore suggests that the relaxation mechanism for the H-bonded proton from the hydroxyl group of the solvent molecule is more efficient than that observed for the α-protons.

Conclusions

The analysis of the powder ENDOR spectrum presented above demonstrates that analysis of powder samples reveals a wealth of spectral information often hidden in an amorphous EPR spectrum. With this technique it should be feasible to examine organic radical species and elucidate the principal hyperfine tensor components. We have extended this analysis to other quinone radicals, and these results will be represented elsewhere. Whereas most investigators of free radicals should benefit from such an analysis, investigation of biological systems should prove to be a particularly fruitful area for future applications.

Acknowledgment. We thank Professor K. C. Hunt for helpful discussions on dipolar interactions and T. K. Chandrashekar for useful discussions and assistance in measuring some of the spectra reported here. This work was supported by the National Institutes of Health (GM 37300), by the Photosynthesis Program of the Competitive Research Grants Office of the U.S. Department of Agriculture, and by the McKnight Foundation.

(33) Yonezawa, T.; Kawamura, T.; Ushio, M.; Nakao, Y. *Bull. Chem. Soc. Jpn.* **1970**, *43*, 1022.

(34) Stone, E. W.; Maki, A. H. *J. Am. Chem. Soc.* **1965**, *87*, 454.

(35) (a) Lubitz, W.; Abresch, E. C.; Debus, R. J.; Isaacson, R. A.; Okamura, M. Y.; Feher, G. *Biochim. Biophys. Acta* **1985**, *808*, 464. (b) Feher, G.; Isaacson, R. A.; Okamura, M. Y.; Lubitz, W. In *Antennas and Reaction Centers of Photosynthetic Bacteria*; Michele-Beyerle, M. E., Ed.; Springer-Verlag: Berlin, 1985; p 174.

(36) Seidel, H. *Z. Phys.* **1961**, *165*, 239.